Study of Turbulent Mixing in a Channel Flow by Numerical Tracking of Material Surfaces

Takahiro Tsukahara[1] & Hiroshi Kawamura[1]

[1]Department of Mechanical Engineering, Tokyo University of Science, Japan

Keywords: Turbulence, Channel flow, Direct numerical simulation, Material surface, Fractals

Abstract: A property of turbulent mixing, i.e. stretching of material surfaces, in a wall-bounded flow is examined through the direct numerical simulation (DNS) of a turbulent channel flow. Statistics of a stretching rate and a fractal dimension on the material surface are presented. A series of DNS has been performed with various initial conditions of the surfaces in order to discuss the influence of the wall on mixing. The stretching rate γ_A, normalized by the Kolmogorov time τ_η, of a material surface in the core region is comparable to that in homogeneous isotropic turbulence. However the asymptotic value for sufficiently extended surfaces is $\gamma_A = 0.1(\tau_{\eta\,\min})^{-1}$ corresponding to one-third of the value $(0.3\,\tau_\eta^{-1})$ for the homogeneous turbulence reported by Goto & Kida [J. Fluid Mech. **586**, 59 (2007)]. The fractal dimension of the surface investigated here through the box-counting procedure increases with time until it attains the asymptotic value of 2.39 ± 0.03.

1. Introduction

The surface separating two fluids in a turbulent flow, even if initially smooth, develops into a complex pattern. For instance, turbulent jets, flames, and cumulus clouds exhibit intricate boundaries. Thus evolutions of material objects in turbulence are of intrinsic interest. Their stretching properties reflect a high potential of transporting and mixing by turbulence. A material object is defined as any line, surface or volume that always consists of the same fluid particles. Tracking of a material surface in turbulence provides important consequences, such as propagations of premixed-flame surfaces, or constant-property surfaces of passive scalars in case of the negligible molecular diffusivity compared to the turbulent mixing.

The passive material objects have been extensively studied by many authors as one of most fundamental topics. The exponential stretching of infinitesimal line and surface elements in homogeneous turbulence was theoretically predicted and numerically confirmed by a number of authors (e.g. Batchelor, 1952; Drummond & Münch, 1990; Girimaji & Pope, 1990; Yeung et al., 1990; Kida & Goto, 2002). Moreover, the stretching rate in length $L(t)$ of finite material line

$$\gamma \equiv \frac{\mathrm{d}}{\mathrm{d}t}\log L(t) \quad \because L(t) = L(0)\exp(\gamma t), \tag{1}$$

and the rate γ_A of surface area $A(t)$

$$\gamma_A \equiv \frac{\mathrm{d}}{\mathrm{d}t}\log A(t) \quad \because A(t) = A(0)\exp(\gamma_A t) \tag{2}$$

are found to be less dependent of the Reynolds number, if it is normalized by the Kolmogorov time, τ_η.This supports the conjecture that small-scale elementary vortices contribute to the exponential evolution in material objects. Recently, Goto & Kida (2007) have reported that the stretching rate of finite-sized material line in the homogeneous turbulence depends on Re; it becomes large at a higher Re. This dependence is caused by the combined effect of various-scale eddies: the folding of material line by large eddies, and the stretching by small eddies.

Much attention was paid to material objects in the homogeneous isotropic turbulence as mentioned above. For finite material lines in a turbulent channel flow, in Tsukahara et al. (2007) we have examined the stretching rate with emphasis on the Reynolds-number dependence and the anisotropic stretching. However, no other study has been done to verify the exponentially stretching of a material surface in a wall-bounded shear flow. In the wall turbulence, the scale of vortical structures is known to range over several orders from the near-wall fine-scale structure to the large-scale one in the outer region, cf. Robinson (1991). In the last two decades, a direct numerical simulation (DNS) of a turbulent channel flow, which is a canonical one of the wall turbulence, has become an important tool in studying the physics of the turbulence structure. However, the influence of the multi-scale eddies and the near-wall viscous effect on the surface evolution are not yet well understood.

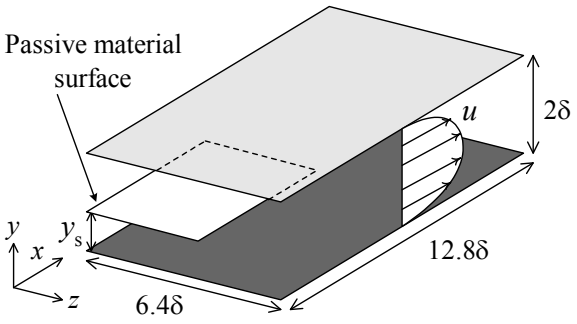

Figure 1. Configuration of channel flow and released material surface at height of y_s. The initial material surface is smooth and parallel to the wall.

The objective of this work is to perform a simulation of the material surface advected in the turbulent channel flow as well as to examine the stretching rate and its fractal geometry in the wall turbulence.

2. Numerical procedure

Lagrangian time series of velocity are obtained from DNS of the fully-developed turbulent channel flow. We solve simultaneously the Navier-Stokes equations for an incompressible flow $\mathbf{u}(\mathbf{x}, t)$ and the advection equation for fluid particles on a material surface as

$$\frac{\mathrm{d}}{\mathrm{d}t}\mathbf{x}_\mathrm{p}(t) = \mathbf{u}\left(\mathbf{x}_\mathrm{p}(t), t\right) \tag{3}$$

with $\mathbf{x}_\mathrm{p}(t)$ the particle position. The mean flow is driven by the uniform pressure gradient in the x direction. The periodic boundary conditions are imposed in the x- and z-directions and the non-slip condition is applied on the walls. Further details of the numerical scheme for the flow field can be found in Abe et al. (2004). The present friction Reynolds number is $\mathrm{Re}_\tau = 180$, which is based on the friction velocity u_τ, the channel half width δ, and the kinematic viscosity ν. The number of grid points is $256 \times 128 \times 256$. The Eulerian statistics calculated from the present DNS are in good agreement with the previous works.

Once the channel flow simulation has reached equilibrium, we start with the particle tracking. Note that a passive material surface is expressed numerically by a set of a number of advecting infinitesimal particles. A segment between two neighboring particles on a material surface generally growths in time. To express a surface smoothly by a set of particle points, all segments must be kept short enough compared to the Kolmogorov scale, η. When a segment exceeds a given threshold $\Delta L \approx \mathrm{O}(\eta_{\min})$ as time progresses, a new particle is inserted at the center of the segment. The calculations are carried out with a number of particle points up to 8×10^6.

3. Result and discussion

3.1. Visualization of temporal evolution

In order to study the effect of the distance from the wall, we performed DNS of material surfaces with four different initial heights of $y_s^+ = 5$, 15, 90 and 180, which correspond to $y_s/\delta = 0.028$, 0.083, 0.5 and 1, respectively

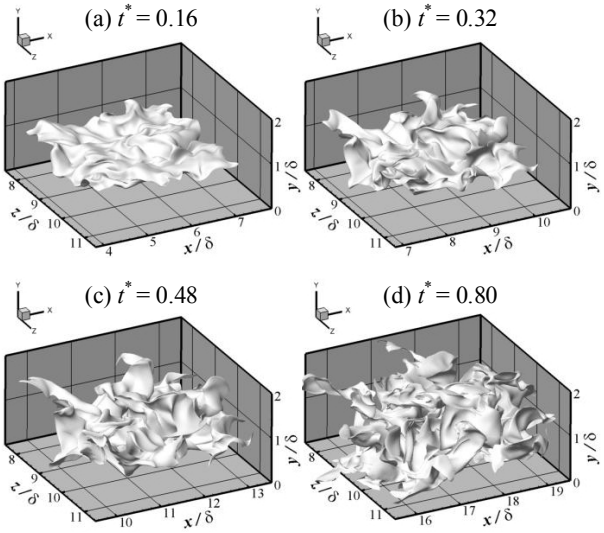

Figure 2. Typical snapshots of a material surface evolving in a turbulent channel flow from time $t^* = 0.16$ to $t^* = 0.80$ for $y_s = \delta$. The surfaces at time t/τ_η = (a) 2.14, (b) 4.28, (c) 6.41, and (e) 10.7, respectively. The mean-flow direction is from left to right.

(here, y_s is referred to as an initial height of a material surface). Figure 2 shows consecutive snapshots of a surface, which starts from $y_s = \delta$ with a flat plane of $3.2\delta \times 3.2\delta$, as it evolves until t^* ($= tu_\tau/\delta$) = 0.96. Here, they are drawn in a portion of the simulation domain. It is observed that the material surface is strongly deformed (stretched and folded many times) by turbulence.

In Fig. 3, we plot the developed material surfaces for other three different initial heights. The time from the start is the same with Fig. 2(b). Some important features may be recognized: (i) the characteristics length of straining depends on the height from the wall; (ii) anisotropic deformation is demonstrated on the surfaces near the wall. The first is predictable because that a material object is convoluted by the Kolmogorov-scale vortex at each height. The second feature is because that, in the buffer layer, the quasi-streamwise vortex is the dominant structure and plays a key role in the mixing of fluid (Robinson, 1991). As one can see, the surfaces in Figs. 3(b) and 3(c) are strongly deformed by turbulence compared to the other case. Whereas the streaky pattern of the deformed surfaces is generated by ejection and sweep in the inner layer, the deformation in the viscous sub-layer is remarkably slow, as shown in Fig. 3(a).

3.2. Stretching rate

Since the area of a material surface tends to increase exponentially in time, its stretching rate, being calculated by Eq. 2, can be well-defined as a roughly constant value. The rates for various initial conditions (height) are plotted as a function of non-dimensional time in Fig. 4.

When the time is normalized by the outer timescale (δ/u_τ), the γ_A for $y_s^+ = 15$ is the largest and rapidly attains some saturation value of $\gamma_A^* = 7.5$ during the early period, as shown in Fig. 4(a). As described above, stretching of material objects is mainly due to the Kolmogorov eddies.

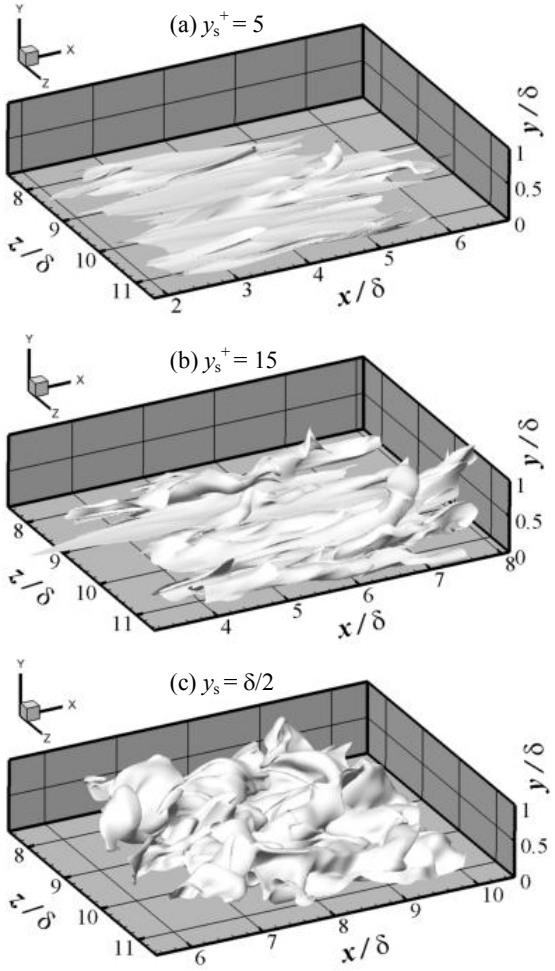

Figure 3. Deformed material surfaces at $t^* = 0.32$ corresponding to (a) $t/\tau_\eta = 20.2$ for $y_s^+ = 5$, (b) 19.5 for $y_s^+ = 15$, and (c) 7.45 for $y_s = \delta/2$, respectively.

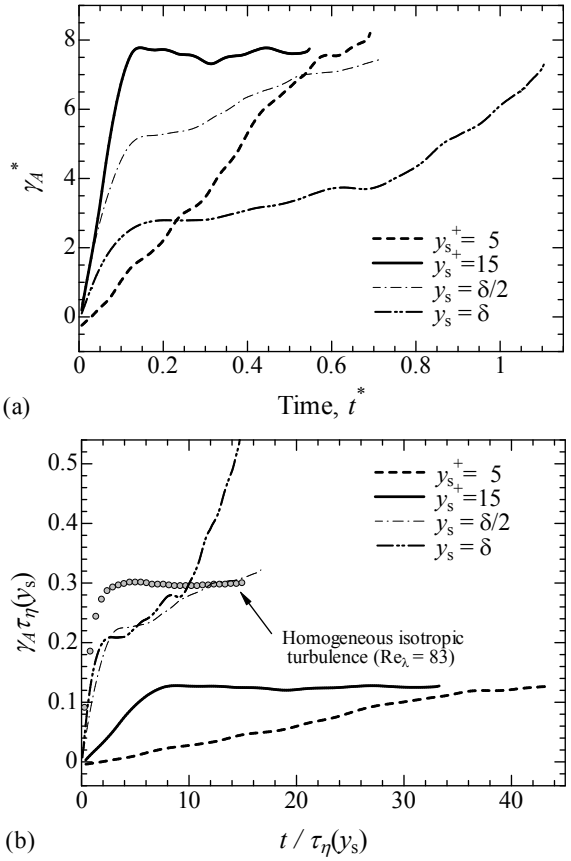

Figure 4. Stretching rate of material surfaces in a turbulent channel flow: the time and the stretching rate are normalized by the outer variable in (a), or by the mean Kolmogorov time τ_η at individual height, in (b). Also shown in the graph (b) is the value for homogeneous isotropic turbulence at the Taylor microscale Reynolds number of 83, from Goto & Kida (2007).

When normalized by the local Kolmogorov time (see Fig. 4(b)), the stretching rates γ_A for $y_s = 0.5\delta$ and δ are indeed less dependent on the height and are comparable to that of homogeneous isotropic turbulence by Goto & Kida (2007). Here we note that, during mixing, the stretching rates undergo continuous transient changes because shear rates vary from location to location. Thus the $\gamma_A \tau_\eta(y_s)$ for the outer-layer case (y_s=0.5δ, δ) keeps increasing in time as the surface evolves into the inner layer, where coherent vortices exist with small length and time scales. On the other hand, the $\gamma_A \tau_\eta$ in the near-wall region (y_s^+=5, 15) are significantly smaller than those in the outer layer. The saturation value normalized by $\tau_\eta(y = 0)$ is about of $\gamma_A = 0.1\,\tau_\eta^{-1}$. In other words, the stretching rate of sufficiently extended surfaces in the turbulent channel is almost one-third of the relevant value ($\gamma_A = 0.3\,\tau_\eta^{-1}$) for homogeneous isotropic turbulence, if it is assumed that the smallest eddies induce the most intensive stretching of surfaces.

3.3. Fractal Dimension

In this section we compute a fractal dimension of a material surface in order to quantify the speed of surface deformation and the complexity of turbulent mixing. A fractal surface generally reveals a dimension greater than 2, but it could have a dimension as high as 3 if it is so highly convoluted as to fill a volume. In this sense, the fractal dimension is a measure of the space-filling ability of a fractal objects. In the box-counting procedure described, for example, in Bergé et al. (1984), one counts the minimum number, $N(\varepsilon)$, of element boxes of size ε required to cover the total area of a total material surface. The dimension of the surface equals to the exponent D in the power law, $N(\varepsilon) \propto 1/\varepsilon^D$. This law holds most fractal objects and follows that

$$D = \lim_{\varepsilon \to 0} \frac{\log N(\varepsilon)}{\log(1/\varepsilon)}, \tag{4}$$

if the limit exists, where D is a so-called box dimension. It can be determined in principle using Eq. 4, but in practice the power law holds only over an intermediate 'scaling range' of ε where $\Delta L << \varepsilon << L_A$. Here, L_A indicates the length scale of a material surface.

Figure 5 shows the variation of $D(\varepsilon)$ given by

$$D(\varepsilon) = \frac{\log N(\varepsilon)}{\log(L_A/\varepsilon)} \tag{6}$$

as a function of ε. As our simulations cover two orders of magnitude of scales, there exists a power-law scaling at $L_A/\varepsilon = 10 \sim 130$, in which a constant value represent the non-integer box dimension of the deformed material surface. The scaling range is roughly comparable to δ/13

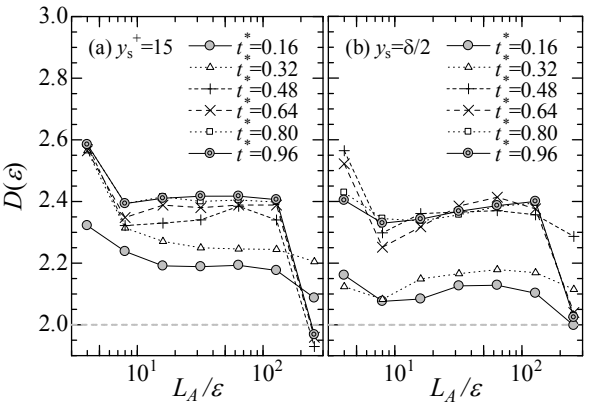

Figure 5. Box-counting data for material surfaces as a function of the inverse of box size ε.

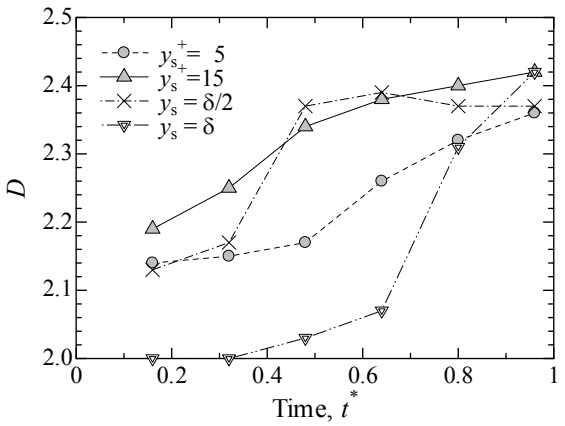

Figure 6. Fractal (box-counting) dimension D of a deformed surface as a function of time.

($= 9\eta_{\min}$) < ε < δ, when the order of L_A is assumed to be O(10δ). It is worth noting that the size of $9\eta_{\min}$ is equivalent to the most expected diameter of the coherent fine-scale eddies (see Tanahashi et al., 2004). On the hand, δ is the order of integral-scale eddies. Therefore, it can be concluded that the stretching of material surfaces and its complex fractal geometry are induced by eddies of various length scales as well as the Kolmogorov-scale eddy. The box dimension D is found to increases with time before attaining its stationary asymptotic value D_∞.

The temporal variations of D for different conditions of y_s are plotted in Fig. 6. The results yields the value $2 < D < 3$, thus a stretched material surface in the wall turbulence is indeed a fractal. It is interesting to notice that D in the case of y_s^+=15 approaches to its asymptotic value faster than those in the other y_s. Such tendency observed in Fig. 6 coincides well with that of γ_A^* in Fig. 4(b), thus indicating a relationship between the fractal dimension and the stretching rate. It can be seen in Fig. 6 that D_∞ is significantly less than 3 and found to be irrespective of the initial condition. The dimension of $D_\infty = 2.39 \pm 0.03$ is quite close to the fractal dimension of scalar interfaces in other classical shear flows, such as jets and wakes, measured by Sreenivasan (1991).

4. Conclusion

We have performed DNS of the turbulent channel flow in which the motion of a material line had been calculated. The stretching rate and the fractal dimension are analyzed with emphasis on the dependence on the initial conditions.

When normalized by the local Kolmogorov time, the stretching rate in the outer layer is scaled irrespectively of the initial condition, which is in agreement with previous work on homogeneous isotropic turbulence. However, the stretching rate of $\gamma_A = 0.1(\tau_{\eta\,\min})^{-1}$ in the inner layer is smaller than that $\gamma_A = 0.3(\tau_{\eta\,\min})^{-1}$ of the homogeneous turbulence by Kida & Goto (2007). We demonstrated that the fractal (box-counting) dimension increase with time, approaching $D_\infty = 2.39 \pm 0.03$ for the fully-developed surface in the channel.

This work was conducted in Research Center for the Holistic Computational Science (Holcs) supported by MEXT. The first author (T.T.) was supported by Japan Society for the Promotion Science Fellowship (18-81).

The simulations were performed with the use of the supercomputing resources at Cyberscience Center of Tohoku University.

5. References

Abe, H., Kawamura, H., & Choi, H. 2004 Very large-scale structures and their effects on the wall shear-stress fluctuations in a turbulent channel flow up to Re_τ = 640. *J. Fluids Eng.*, Vol. 126, pp. 835-843.

Batchelor, G. K. 1952 The effect of homogeneous turbulence on material lines and surfaces. *Proc. R. Soc. Lond. A*, Vol. 213, pp. 349-366.

Bergé, P., Pomeau, Y. & Vidal, C. 1984 *Order within Chaos*, Wiley, New York.

Drummond, I. T. & Münch, W. 1990 Turbulent stretching of line and surface elements. *J. Fluid Mech.*, Vol. 215, pp. 45-49.

Girimaji, S. S. & Pope, S. B. 1990 Material element deformation in isotropic turbulence. *J. Fluid Mech.*, Vol. 220, pp. 427-458.

Goto, S. & Kida, S. 2007 Reynolds-number dependence of line and surface stretching in turbulence: folding effects. *J. Fluid Mech*, Vol. 586, pp. 59-81.

Kida, S. & Goto, S. 2002 Line statistics: Stretching rate of passive lines in turbulence. *Phys. Fluids*, Vol. 14, pp. 352-361.

Robinson, S. K. 1991 Coherent motions in the turbulent boundary layer,. *Annu. Rev. Fluid Mech.*, Vol. 23, pp. 601-639.

Sreenivasan, K. R. 1991 Fractals and multifractals in fluid turbulence. *Annu. Rev. Fluid Mech.*, Vol. 23, pp. 539-600.

Tanahashi, M., Kang, S.-J., Miyamoto, T., Shiokawa, S. & Miyauchi, T. 2004 Scaling law of fine scale eddies in turbulent channel flows up to Re_τ = 800. *Int. J. Heat and Fluid Flow*, Vol. 25, pp. 331-340.

Tsukahara, T., Iwamoto, K. & Kawamura, H. 2007 Evolution of material line in turbulent channel flow. *Proc of TSFP5*, pp. 549-554.

Yeung, P. K., Girimaji, S. S. & Pope, B. 1990 Straining and Scalar Dissipation on Material Surfaces in Turbulence: Implications for Flamelets. *Comb. and Flame*, Vol. 79, pp. 340-365.